

Clinical Manifestations and Medical Imaging of Osteogenesis Imperfecta: Fetal Through Adulthood

Jennifer S. Weaver¹, Jonathan W. Revels¹, Jamie M. Elifritz¹, Benjamin Whitlow¹, Michele Retrouvey², Sherry S. Wang³

¹University of New Mexico, Department of Radiology, ²Eastern Virginia Medical School, Department of Radiology,

³University of Utah, Department of Radiology and Imaging Sciences

Correspondence: jsweaver@salud.unm.edu; Tel.: + 1 734 717 6878; Fax.: + 1 505 272 5821

Received: 17 February 2021; **Accepted:** 27 May 2021

Abstract

The aim of this paper is to describe the varying clinical and imaging manifestations of Osteogenesis Imperfecta (OI) in the fetus, the child, and the adult. OI is a genetic disorder with mutation of Type 1 and non-type 1 collagen genes that results in disruption of multiple collagen based organ systems, most notably bones, often leading to “brittle bones”. Additional features such as blue sclera, dentinogenesis imperfecta, joint and ligamentous hyperlaxity, hearing loss and cardiac defects may be present. Currently, there are at least 30 recognized genetic forms of OI. Given the multiple genes involved, variable genetic inheritance, and the wide range in phenotype, diagnosis can be challenging. While OI may sometimes be diagnosed in the fetus, patients with mild forms of OI may be diagnosed in childhood or even in adulthood. Imaging, including ultrasound, radiography, computed tomography, and magnetic resonance imaging, plays an important role in the diagnoses of OI in the fetus, the child, and the adult. Imaging is also crucial in identifying the many multisystem manifestations of OI. In particular, imaging can help differentiate manifestations of OI from injuries sustained in non-accidental trauma. Age, severity and manner of presentation of OI vary broadly depending on the specific genetic mutation involved, mode of inheritance, and age of the patient. Successful diagnosis of OI hinges on a detailed knowledge of the variable presentation and complications that may be encountered with this disease. **Conclusion.** In conclusion, OI comprises a heterogeneous group of genetic disorders responsible for bone fragility and additional connective tissue disorders, which can result in specific clinical and imaging findings in the fetus, the child, and the adult.

Key Words: Osteogenesis Imperfecta ▪ Magnetic Resonance Imaging ▪ Ultrasound.

Introduction

Osteogenesis imperfecta (OI) is a rare genetic disorder that results in fragile bones (1). The pro-alpha 1 and pro-alpha 2 chains, which make up type 1 collagen, are encoded by the *COL1A1* or the *COL1A2* genes (2). The mutation of these genes results in the various clinical symptoms. Although it has been classically taught that OI encompasses multiple subtypes of a genetic disease that affect type 1 collagen fibers, as the understanding of this disease grows, it is now known that multiple non-type 1 collagen gene alterations exist. As a result of these genetic abnormalities, patients possess weakness in multiple collagen-based organ sys-

tems, most notably bones. The decreased osseous strength is due to a combination of both poor bone mineral density and overall poor quality from abnormal osseous matrix formation (3) which leads to increased risk for fracturing that may occur in utero, postnatal, and beyond into adulthood. In normal bones, stiffness which prevents bending of bone from body weight, toughness which allows energy absorption during impact, and strength which is the load bearing capacity of bone combine to prevent fracture (4, 5). With OI, abnormal bone with low bone mass and increased mineral concentration leads to abnormal bone matrix and microstructure and overall increased fragility and disrupted fracture repair (4, 5).

While OI may sometimes be diagnosed in utero, patients with mild forms of OI may escape diagnosis until childhood or even in adulthood. Imaging plays an important role in the diagnoses of OI in the fetus, the child, and the adult, as well as identifying the many multisystem manifestations of OI. In children, imaging is important in differentiating OI from non-accidental trauma (NAT), which is physical abuse purposefully imposed on an infant or child, also commonly referred to as “child abuse” or “shaken baby syndrome”.

There is a high variability of clinical symptoms associated with OI which vary with subtype, the most common of which are frequent fractures and bone deformities. Other common symptoms include blue sclera, short stature, dentinogenesis imperfecta, and hearing loss. Several current imaging modalities play an important role in the diagnosis and management of patients with OI, and several new imaging methods are on the horizon (6, 7) (Table 1).

Table 1. Imaging of OI.

Modality	Clinical Indications	Advantages	Disadvantages and Limitations
Radiography	<ul style="list-style-type: none"> - Fractures - Bone deformities - Estimate of bone mineral density 	<ul style="list-style-type: none"> - Inexpensive - Widely available 	<ul style="list-style-type: none"> - Ionizing radiation - Low fracture sensitivity in severe osteopenia - Skeletal deformity and fragility may limit positioning
Dual Energy X-ray Absorptiometry (DXA)	<ul style="list-style-type: none"> - Assessment of bone mineral density 	<ul style="list-style-type: none"> - Relatively widely available 	<ul style="list-style-type: none"> - Ionizing radiation (low) - Relatively expensive - Complicated interpretation with fractures, hardware, bone deformities, and low body height
Ultrasound	<ul style="list-style-type: none"> - Prenatal assessment 	<ul style="list-style-type: none"> - No ionizing radiation - Portable - Widely available - Relatively inexpensive 	<ul style="list-style-type: none"> - Operator dependent
Computed Tomography (CT)	<ul style="list-style-type: none"> - Fracture - Bone deformities - Preoperative assessment and planning 	<ul style="list-style-type: none"> - 	<ul style="list-style-type: none"> - Expensive - Ionizing radiation - May not be widely available - Skeletal deformity and fragility may limit positioning
Magnetic Resonance Imaging (MRI)	<ul style="list-style-type: none"> - Fracture - Bone deformities - Preoperative assessment and planning - Fetal evaluation 	<ul style="list-style-type: none"> - No ionizing radiation - High soft tissue resolution 	<ul style="list-style-type: none"> - Expensive - Long examination time - May be contraindicated in patients with severe claustrophobia - Contraindicated with certain implanted devices - May not be widely available - Skeletal deformity and fragility may limit positioning
Peripheral Quantitative Computed Tomography (pQCT)	<ul style="list-style-type: none"> - Assessment of bone mineral density, bone microstructure, and bone morphology in the peripheral skeleton 	<ul style="list-style-type: none"> - Rapid image acquisition - Portable - Inexpensive - Allows multiple site assessment 	<ul style="list-style-type: none"> - Ionizing radiation (very low) - Limited availability clinically - May be limited by bone deformity
High-resolution pQCT (HR-pQCT)	<ul style="list-style-type: none"> - Assessment of bone mineral density, bone microstructure, and bone morphology in the peripheral skeleton 	<ul style="list-style-type: none"> - Rapid image acquisition - Allows multiple site assessment 	<ul style="list-style-type: none"> - Ionizing radiation (very low) - Limited availability clinically - May be limited by bone deformity - Expensive - Not portable
Slit Beam Digital Radiography	<ul style="list-style-type: none"> - Assessment of skeletal alignment and deformity 	<ul style="list-style-type: none"> - Lower radiation dose than CT and radiographs - 3D reconstruction 	<ul style="list-style-type: none"> - Long acquisition times may have increased motion artifact, especially in children - Skeletal deformity and fragility may limit positioning - Limited availability
Quantitative Ultrasound (QUS)	<ul style="list-style-type: none"> - Assessment of bone quality and bone mass 	<ul style="list-style-type: none"> - Ultrasound widely available 	<ul style="list-style-type: none"> - Limited data available

The aim of this paper is to describe the varying clinical and imaging manifestations of OI in the fetus, the child, and the adult. This paper also aims to describe several imaging modalities used in evaluation of patients with OI, including several important recent advancements in imaging.

OI: Subtypes

At present there are at least 30 recognized genetic forms of OI and their subtype classification has grown beyond the Sillence scheme developed in 1979 where patients were grouped into 4 subtypes based on their disease severity, mild to lethal. It is important to recognize that the increase in numer-

ical value does not correlate with disease severity (3, 8) (Table 2). In 2015 the Nosology Group of the International Skeletal Dysplasia Society added OI subtype V to the 4 subtypes originally described by Sillence (9). The phenotypically based Sillence classification was preserved in the 2019 revision of the Nosology (10).

A more modern approach to OI classification takes into consideration the underlying genetic abnormality (specific gene and role in abnormal collagen synthesis), while still maintaining parts of the Sillence classification system (3) (Table 3).

In the modern classification system of OI, the majority of OI subtypes fall into group A, including the original Sillence subtypes I-IV, and possess

Table 2. Sillence Classification of OI

Type	Clinical severity	Example features	Life expectancy
I	Mild deformity	Mildly short stature or normal height; blue sclera	Full life span.
II	Perinatal lethality	Intrauterine rib and long bone fractures; hypodense skull	Typically stillborn, or death within the first two months of life
III	Severe deformity	Severely short stature/dwarfism; severe spinal scoliosis	Typically full life span. Many develop severe neurological and/or respiratory complications in childhood due to bone weakness and fragility
IV	Moderate deformity	Moderately short stature; mild to moderate scoliosis	Full life span

Table 3. OI Classifications Based on Genetic Mutations While Still Maintaining Some Features of the Sillence Classification

Group	Subtype	Gene(s)	Mechanism
A	I	<i>COL1A1</i> or <i>COL1A2</i>	Defective collagen synthesis, processing, and structure formation
	II	<i>COL1A1</i> or <i>COL1A2</i>	
	III	<i>COL1A1</i> or <i>COL1A2</i>	
	IV	<i>COL1A1</i> or <i>COL1A2</i>	
	XIII	<i>BMP1</i>	
B	VII	<i>CRTAP</i>	Defective post-translational modification of collagen
	VIII	<i>LEPRE1</i>	
	IX	<i>PPB</i>	
	XIV	<i>TMEM38B</i>	
C	X	<i>SERPINH1</i>	Defective collagen folding and/or crosslinking
	XI	<i>FKBP10</i>	
	-	<i>PLOD2</i>	
	-	<i>P4HB</i>	
D	V	<i>IFTM5</i>	Defective bone mineralization
	VI	<i>SERPINF1</i>	
E	XII	<i>SP7</i>	Defective osteoblast differentiation
	XV	<i>WNT1</i>	
	XVI	<i>CREB3L1</i>	

a mutation in the *COL1A1* and *COL1A2* genes resulting in reduced collagen production and poor fiber assembly (3). Nearly all of group A subtypes are inherited in an autosomal dominant fashion, in comparison to the remaining groups where autosomal recessive inheritance predominates (3). Group B mutations result in poor post-translation modification of collagen, resulting in severe subtypes of OI that typically present in infancy (3). Group C patients possess mutations that would normally regulate collagen folding and crosslinking causing moderate to severe forms of OI (3). One syndromic form of OI that falls into Group C is Cole-Carpenter syndrome which in addition to OI includes craniosynostosis, proptosis, hydrocephalus, and abnormal facial features (3, 11). Group D subtypes of OI involve abnormalities in bone mineralization, both increased and decreased (3). Lastly, group E subtypes possess genetic mutations that affect osteoblast differentiation (3). Screening for mutations at these gene locations are useful for diagnosis. Furthermore, genetic testing for the parents may also uncover genetic mutations in an asymptomatic parent.

OI in Fetus

Ultrasound (US) is the main modality for the in-utero diagnosis of OI, which may be discovered on the routine anatomical survey around 20 weeks of gestation. However, the varied phenotype and severity of

skeletal dysplasia makes it difficult to diagnose accurately with only 65% of suspected OI diagnoses made on prenatal US found to be accurate (12). OI types I and IV are generally mild without many bone fractures, and variable degrees of hearing loss and dentinogenesis imperfecta. Type II is a lethal form and type III is progressive with short stature, dentinogenesis imperfecta, and hearing loss. US has been shown to be helpful in the diagnosis of Type II and deforming type III OI (13). US features of OI include short extremities, bone fractures/increased bone plasticity, and decreased mineralization with decreased echogenicity of the skeletal structures (14) (Figure 1). Less specific findings such as intrauterine growth retardation or hydramnios may also be present. 3 dimensional (3D) rendering US has been shown to help improve diagnosis and disease detection (15) and to

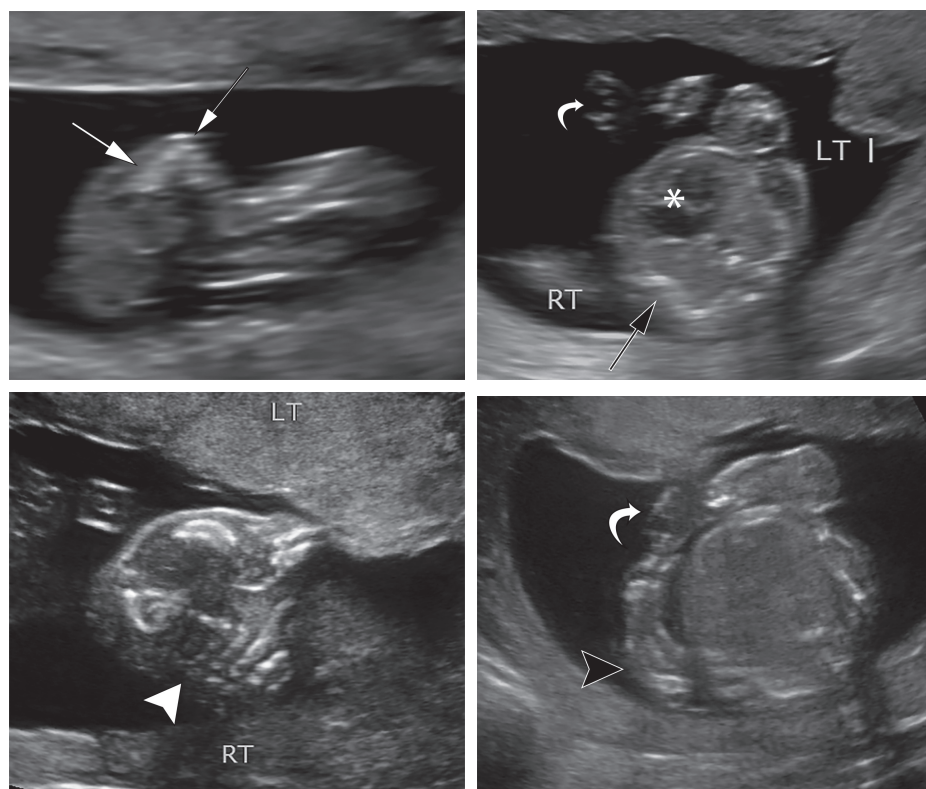


Figure 1. Fetal US images of a 20 week 4 day intrauterine demise secondary to OI. (A) Right femur deformity (white arrow) with bending at the diaphysis indicating fracturing. (B) Multiple right rib fracture deformities (black arrow) in transverse axis (heart denoted by *, umbilical cord by curved arrow for orientation). (C) Same rib fractures (white arrowhead) in long axis. (D) Right radius/ulna with bending (black arrowhead) at the diaphysis indicating fracturing (foot denoted by curved arrow for orientation).

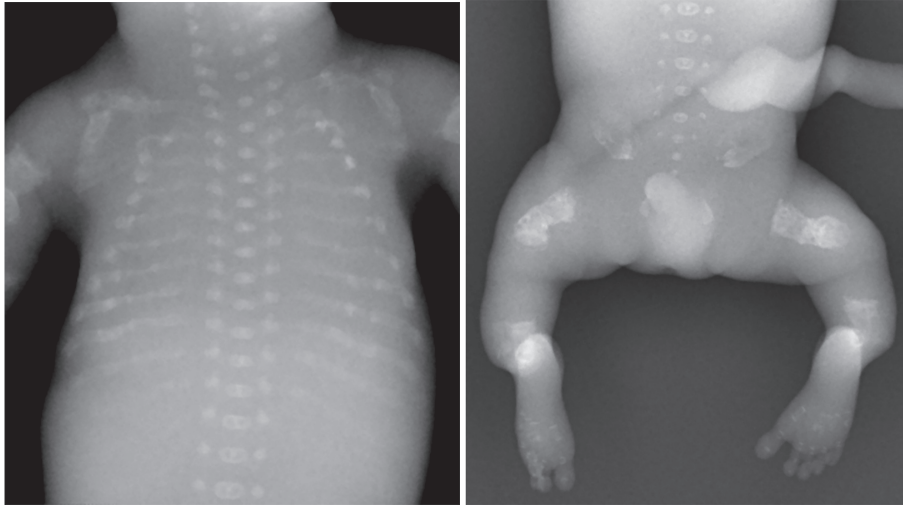


Figure 2. Postmortem radiographs of fetus in Figure 1. Radiographs of the chest (A) and pelvis/lower extremities (B) show multiple rib and long bone fractures.



be superior when used in adjunct with 2D US in the prenatal diagnosis of fetal anomalies (Figure 1). Postmortem radiographs are important adjuncts to confirming and specifying the fetal bone abnormalities in lethal cases of OI (Figure 2).

On prenatal US, OI lethality risk stratification can be performed by multiple means by comparing femur length, abdominal circumference, and chest circumference. Femur length to abdominal circumference ratio of less than 0.16 represents a lethal skeletal dysplasia in 92-96% of cases (16). When this finding is combined with polyhydramnios, the ability to predict lethality can be as high as 100% (16). Chest circumference to abdominal circumference ratio of less than 0.6 represents a lethal skeletal dysplasia in 86.4% of cases (17).

In cases of doubtful diagnosis of OI on prenatal US, low dose computed tomography (CT) with 3D reconstructions can be helpful in assessment of the entire fetal skeleton, performed after 26 weeks of gestation to aid diagnostic accuracy (18) (Figure 3).

The role of magnetic resonance imaging (MRI) is limited but this imaging modality can be useful for assessment of associated abnormalities and the fetal lung volume which can stratify lethality (Figure 4). While MRI has many advantages, such as no

Figure 3. Low dose CT 3D reconstructions of a second trimester fetus of a mother with history of OI. (A, B) Fetal rib (arrowhead) and femoral (arrows) fractures. The mother (C) also has chronic pelvic deformities and a right femoral fracture.

ionizing radiation and high soft tissue resolution, it also has many limitations, such as long examination times, expense, and safety considerations when implanted medical devices are present.

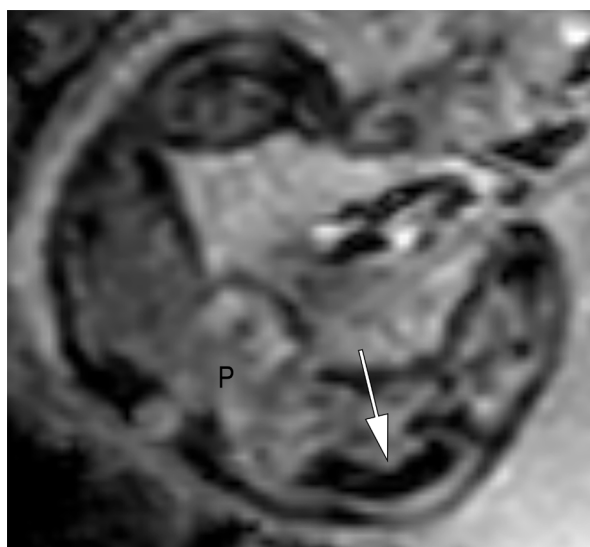


Figure 4. Fetal echo planar MR image of a 31 week 1 day old fetus with OI, showing angulation of the femur (arrow) (pelvis denoted by P for orientation). (Image courtesy of Katherine Epstein, MD)

Regardless of imaging modality used, it is important to look for associated abnormalities that can be seen in OI. Rare anomalies that have been previously described in the literature include microcephaly (19), congenital heart defects (19), anencephaly (20), and encephalocele (21). Given the rarity of the aforementioned neurologic and cardiac abnormalities amongst OI cases, their incidence and order of prevalence is difficult to determine.

OI in Infancy and Childhood

The clinical presentation of OI in newborns, neonates and children is highly variable in both features and severity. The most common abnormalities include osteoporosis with increased osseous fragility, blue sclera, dentinogenesis imperfecta, and hearing impairment. Other features include ligamentous laxity, hypermobility of the joints, short stature and vascular fragility leading to easy bruising. There is known association of OI with

congenital cataracts (22). The diagnosis is most commonly made at birth, but in the diagnosis of milder forms such as OI type I, can be delayed well past age 4 years (23).

Radiography is the preferred initial modality for the assessment of OI in pediatric patients. The main radiographic features of OI are osteopenia, bone fractures, and bone deformities. The bones may be profoundly osteopenic with cortical thinning and increased lucency at the medullary cavity due to rarefaction of the trabeculae. However, osteopenia is often difficult to accurately diagnose on radiographs, as images may appear normal until ~50% of the bone has been lost (18). Dual energy x-ray absorptiometry (DXA) is a sensitive imaging modality to assess and monitor osteopenia. However, the presence of osseous fractures and deformities, orthopedic hardware, and low body height in OI can make DXA evaluation difficult in patients with OI (24). It is important to remember that osteopenia is not specific for OI and can be seen in variety of metabolic disorders (18).

Multiple fractures are a hallmark of OI, affecting both the axial and appendicular skeleton. Fractures may be caused by minimal trauma but are similar in distribution to those in healthy children, most commonly affecting the diaphysis of the long bones. The callus associated with healing may be hyperplastic, particularly in OI type V (25) (Figure 5). These findings are not specific to OI and can be seen in NAT, more so when there is calcification of a healing subperiosteal hematoma. Hyperplastic osseous calluses can also be seen in cases of spinal dysraphism, bleeding disorders and neurofibromatosis (18). Pseudoarthrosis may develop at the site of healing fractures and bones may become deformed (Figure 6).

Axial skeletal abnormalities in cases of OI include calvarial enlargement, Wormian bones (subset of the small intrasutural ossification centers interposed between the cranial sutures) (Figure 7), delayed closure of the fontanelle, scoliosis, vertebral compression fractures, codfish vertebrae, as well as basilar invagination (invagination of the base of the skull with the top of the C2 vertebra migrated upward which may cause narrowing of

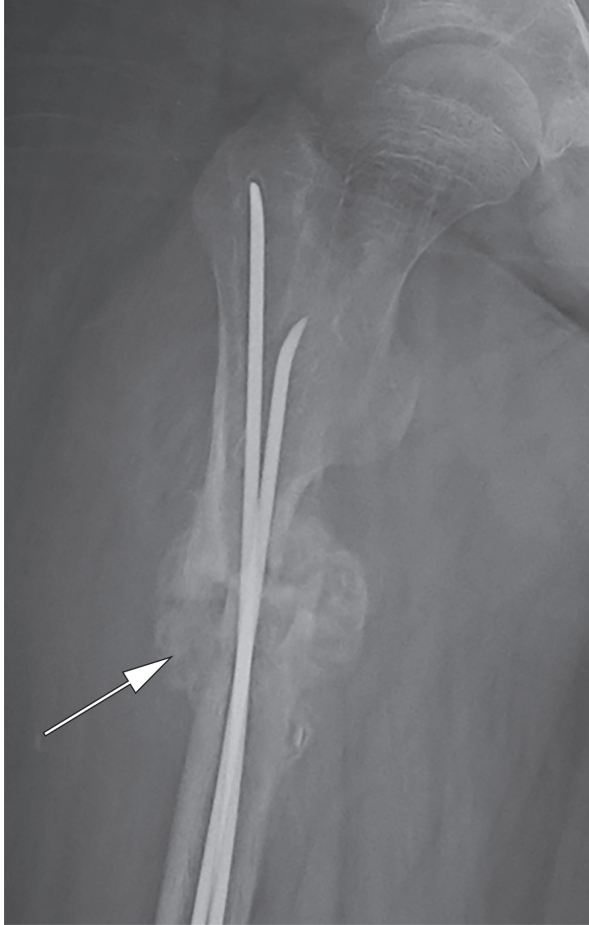


Figure 5. Frontal radiograph of the femur in a 13 year old with OI, demonstrating hyperplastic callus at a mid-femoral fracture, transfixed with two flexible intramedullary nails.

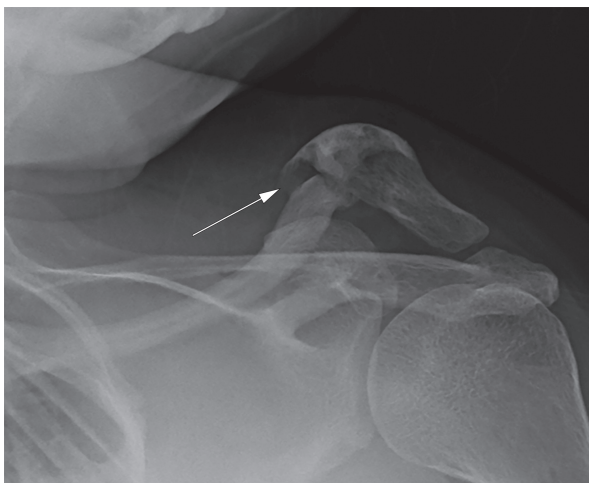


Figure 6. Frontal radiograph of the left clavicle in a 28 year old with OI, with a pseudoarthrosis at the site of prior fracture.

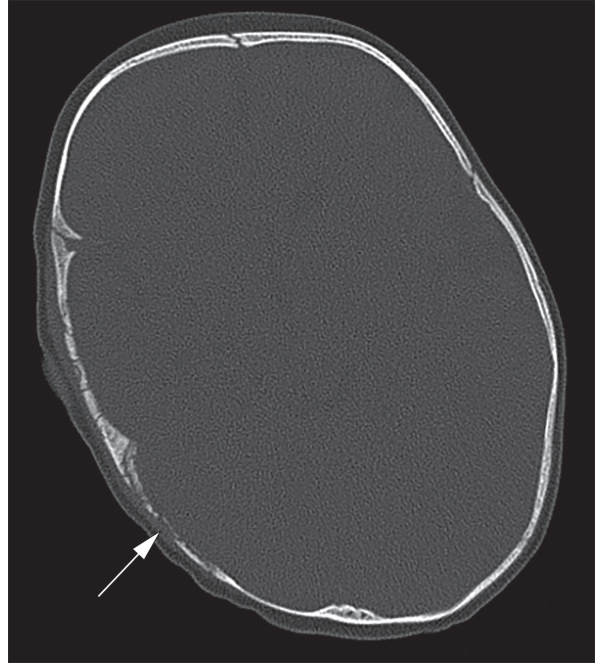


Figure 7. Axial CT image of the head in a 7 month old with OI shows multiple small bones along the right lambdoid suture, consistent with Wormian bones.

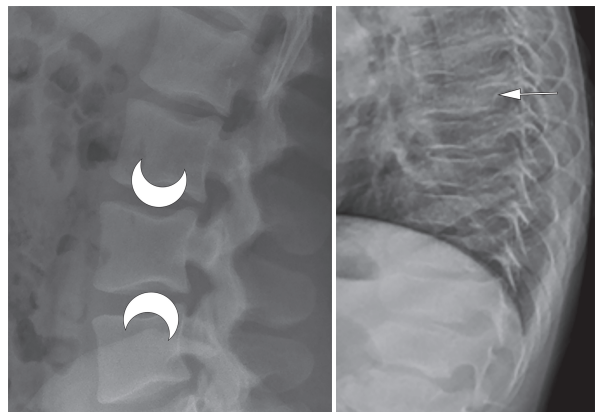


Figure 8. Lateral lumbar spine radiograph in patient 24 year old with OI (A) shows multiple biconcave (codfish) vertebral bodies. A lateral thoracic spine radiograph (B) in a 6 year old with OI shows platyspondyly (multiple flattened vertebral bodies).

the foramen magnum), and platyspondyly (Figure 8, 9). Pectus excavatum or carinatum may be seen, as well as coxa vara (Figure 10). In the appendicular skeleton, bowing and gracile appearance of the long bones is frequent (Figure 11).

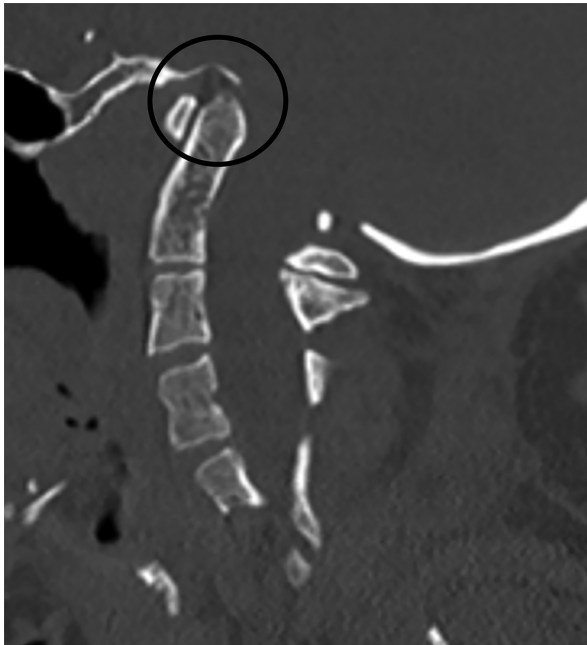


Figure 9. Sagittal CT of the cervical spine in a 34 year old with OI showing basilar invagination with proximal migration of the dens (black circle).

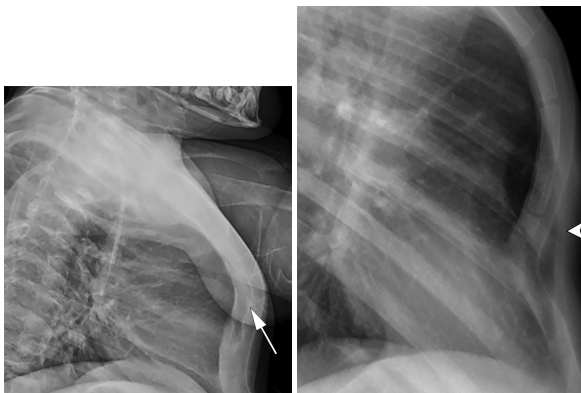


Figure 10. Lateral chest radiographs showing sternum protruding anteriorly (A) in an 8 year old with OI with pectus carinatum and (B) depressed in a 15 year old patient with OI with pectus excavatum.

In younger children, the long bones may demonstrate a “bamboo cane appearance”, where bones are thick and broad with lack of osseous remodeling. Children with type OI may have scalloping at the bone metaphyses and epiphyses with popcorn calcifications, most commonly in OI type III (Figure 12). This tends to occur in the metaphyseal and epiphyseal regions of the knee and may result in leg length discrepancy (26).



Figure 11. Lateral radiograph of the tibia/fibula, showing long bone bowing in a 4 year old with OI.

Cyclic administration of bisphosphonates is often used as treatment for OI. Bisphosphonates can induce the formation of dense metaphyseal bands and occasionally epiphyseal and apophyseal bands, secondary to failure of remodeling of the primary to secondary spongiosa at the physis, creating the “zebra stripe sign” (27-31) (Figure 13). When these lines are present, care should be taken that bone mineralization density is not overestimated on imaging.



Figure 12. Frontal shoulder radiograph of a 14 year old with type 3 OI, showing coarse “popcorn” calcifications within the left proximal humeral metaphysis.

Postnatal CT is usually not necessary, but may be helpful to better assess Wormian bones (Figure 7). Otosclerosis is best evaluated with a temporal bone CT (32). Basilar invagination may be identified on cervical spine CT and MRI (Figure 9).

In a pediatric patient that presents with multiple fractures, there are several differential considerations, including OI, particularly type I and IV, as these patients may have near normal bone mineralization. However, the most common cause of multiple injuries remains NAT (33, 34). There is considerable overlap between fractures that occur due to accidental trauma and NAT and certain fractures have been found to be highly specific for NAT. Metaphyseal corner fractures are thought to be due to shearing of the weak metaphysis in the growing child when the child is shaken and as such are thought to be pathognomonic of NAT (Figure 14). Rib fractures are not particularly common in OI, but they are often seen in NAT, particularly at the posterior ribs, thought to be related to the anteroposterior compression of the rib cage as the child is shaken (22) (Figure 15).

Skull fractures are common in accidental trauma and NAT, but are not particularly common in OI. Additional findings that raise concern for NAT

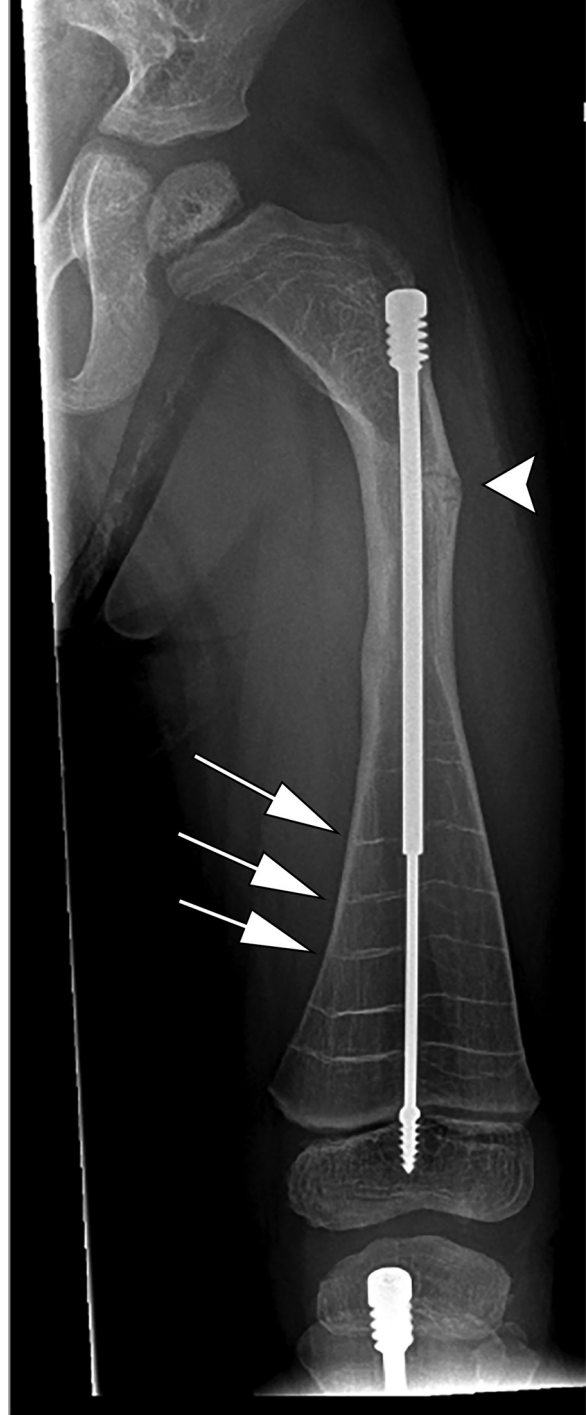


Figure 13. Frontal radiograph of the femur in a 5 year old with Type 4 OI shows an intramedullary nail transfixing the femur, with a healing fracture (arrowhead) of the proximal lateral femoral cortex. Multiple alternating dense (white arrows) and lucent bands are present in the metaphysis (“zebra stripe sign”), presumably due to cyclic bisphosphonate therapy.

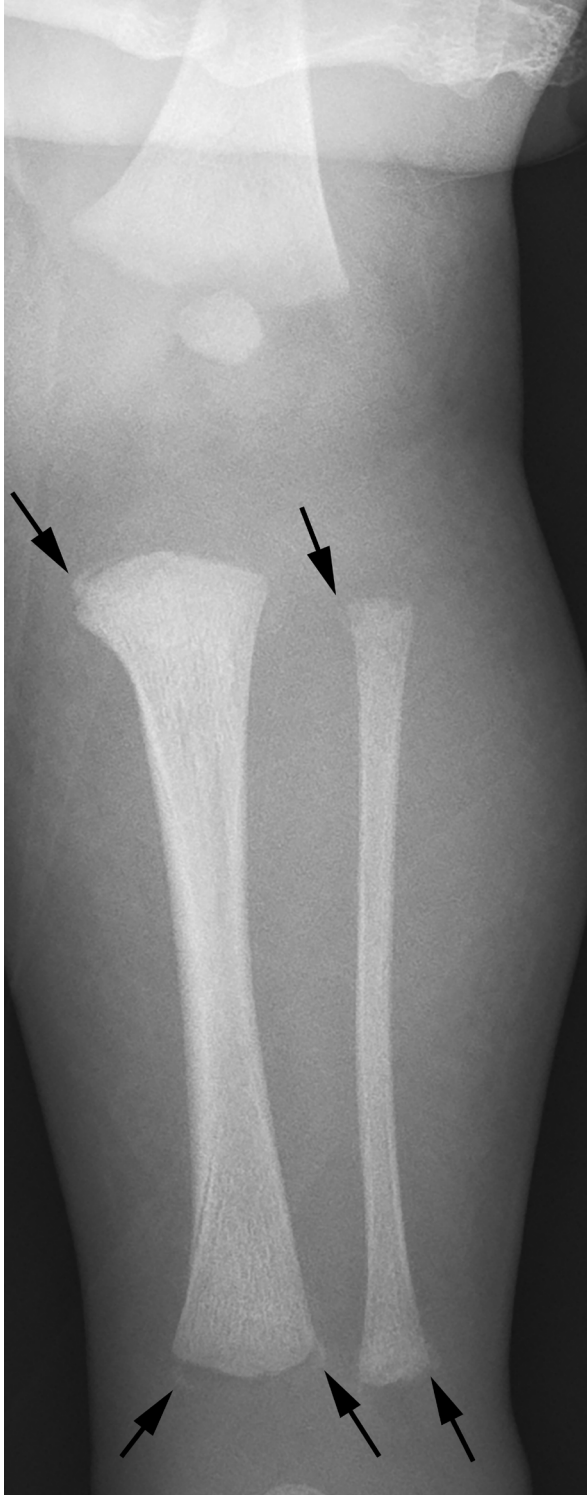


Figure 14. Frontal radiograph of the tibia and fibula in an 11 day old neonate with NAT, showing proximal and distal metaphyseal "corner" fractures (arrows) in the tibia and fibula with extensive soft tissue swelling.



Figure 15. Frontal radiograph of the chest in an 11 day old neonate with NAT, showing posterior rib fractures (arrows).

includes multiple skull fractures or fractures that involve more than one bone or cross sutures, as well as depressed skull fractures. Diastatic sutures are also associated with NAT. Scapular and sternal fractures, as well as distal clavicular fractures are suggestive of NAT and not commonly seen with OI (33). NAT disproportionately affects very young children. In the 1980s it was found that nearly one-third of all cases occurred before 6 months of age, one-third occurred between 6 months and 3 years and one-third occurred in children over the age of three (35).

Other differential considerations when presented with a patient with multiple fractures may include osteopenia of prematurity, osteomalacia, juvenile osteoporosis, hypophosphatemia, Rickets, copper deficiency, scurvy, and Menkes syndrome.

OI in Adults

Rarely, very mild forms of OI may remain undetected until adulthood and may be diagnosed incidentally following a fracture. OI should be considered in the differential diagnosis for an adult with an unexplained fracture, prior to expected age-related osteoporosis and without any known disease that may lead to osteoporosis. Additional differential considerations for unexplained adult

fractures include Gaucher disease, Marfan syndrome, hypophosphatemia, and various causes of hypogonadism (36).

Recent research has focused on improving the characterization of OI in adulthood, particularly mild forms of OI, which has previously been poorly understood relative to pediatric OI. Increased awareness and continued improved treatment of OI in recent years have contributed to progressively increased life expectancy and quality of life in OI patients.

Radiographs remain the primary modality for diagnosis and follow-up of fractures in adult OI patients. As in children, the primary and least variable symptom of OI in adults is brittle bones. Fracture rates decline with skeletal maturity; however, approximately 25% of OI-related fractures occur in adults (37). In ambulatory adults, fractures of the vertebral bodies, hips, and feet are common, with as many as 50% of fractures involving the spine (37).

Serial radiographs are useful in these patients to evaluate fracture healing, while additional imaging such as CT may be of use if intervention is planned. Manifestations of OI in adults are highly variable, and are not limited to brittle bones and frequent fractures; the multisystem manifestations of OI are often of concern (38).

Fractures in adults with OI may present additional challenges to the orthopedic surgeon relative to the general population. While OI does not prolong fracture healing, OI patients have higher rates of malunion and nonunion, and up to 20% of OI patients experience nonunion of at least one fracture (37). Nonsurgical management of fractures is often preferred. Hip arthroplasties are associated with a higher complication rate in patients with OI, and vertebroplasties are generally contraindicated in treatment of spinal fractures due to high risk of cement extravasation (37). There are several additional musculoskeletal manifestations of OI in adults. These may be diagnosed incidentally on radiographs following a fracture or by MRI for evaluation of musculoskeletal pain. Not infrequently, acetabular protrusio can be seen in adult patients with OI (Figure 16). Osteoarthritis is common,

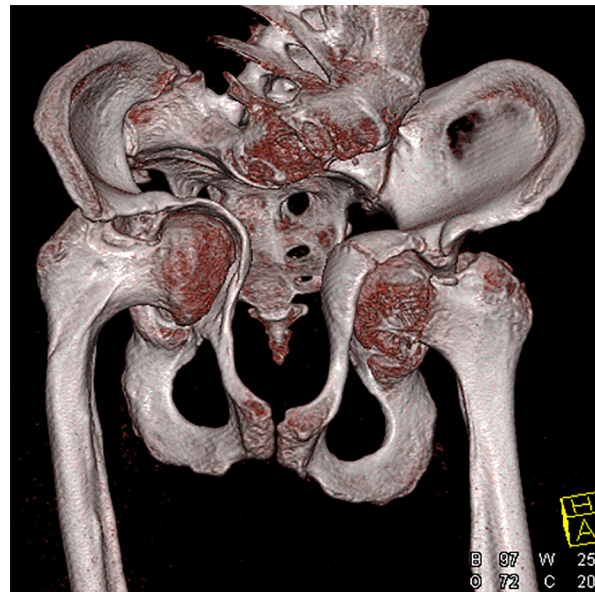


Figure 16. Frontal pelvis radiograph (A) and 3D CT reconstruction (B) of the pelvis in a 45 year old patient with Type 4 OI, demonstrating osteopenia, lumbar scoliosis, and severe bilateral acetabular protrusio.

with nearly half in an online survey of adults by the OI Foundation reporting a formal diagnosis of arthritis (39). Post-traumatic osteoarthritis is also common and the periarticular bone dysplasia and subchondral insufficiency may contribute to rapid progression of osteoarthritis (37). Joint laxity is relatively common, and some patients may benefit from assistive devices originally developed for management of Ehlers-Danlos Syndrome (36). Tendinopathy and tendon rupture may also occur.

This has been less well characterized and overall prevalence is unknown; however, approximately one third of patients in the OI Foundation survey reported prior tendon rupture (39). MRI and diagnostic ultrasound may be useful if tendon pathology is suspected.

Nontraumatic spinal pathologies, including kyphoscoliosis and spondylolisthesis, are more common in adults with OI compared with the general population. Progressive spinal deformity may exacerbate pulmonary dysfunction particularly in more severe forms of OI. Craniocervical junction abnormalities, including basilar invagination, basilar impression, and platybasia, are also seen, more commonly in severe OI. Lateral radiographs of the cervical spine remain most useful in diagnosis of craniocervical abnormalities, while CT may help better evaluate osseous structures (Figure 8, 9).

The most severe craniocervical junction abnormality, basilar impression, typically presents with nonspecific neurological symptoms including headache, vertigo, torticollis, and abnormal reflexes (Figure 9). Rapid diagnosis and treatment are important, as untreated basilar impression may lead to severe neurological consequences including paralysis and death. As with other craniocervical junction abnormalities, radiographs and CT are useful for characterization of osseous structures, while MRI should be considered for better evaluation of neurological structures if basilar impression is suspected.

Dentinogenesis imperfecta is common in patients with OI because part of the dentine of teeth is made up of type 1 collagen resulting in brittle yellow-brown teeth that are at risk of fracturing, decay, and infection (40). Presence of dentinogenesis imperfecta is variable, and the association between dentinogenesis imperfecta and collagen gene mutations is poorly understood. Diagnosis of dentinogenesis imperfecta is often made using clinical and radiographic findings. Dental infection may rarely exacerbate or lead to osteonecrosis of the jaw in patients receiving bisphosphonate therapy.

Hearing loss affects approximately 48-72% of adult OI patients (41). This is most commonly

conductive type with symptoms beginning at the second through fourth decades of life, and later progressing to a mixed type (conductive and sensorineural) (41). CT and MRI of the temporal bone may be of use in evaluating hearing loss in OI to assess for otosclerosis.

Cardiovascular disease is common in adults with OI, often after age 40 and includes aortic and mitral insufficiency, heart failure, and aortic root dilation (42). Hypertension is seen in up to 40% of adults with OI (37) and may be exacerbated by frequent NSAID treatment of musculoskeletal conditions as well as physical inactivity that may be secondary to musculoskeletal deformities.

New Horizons in Imaging of Patients with OI

There have been several important recent advancements in imaging that are useful in evaluating patients with OI, to include peripheral quantitative computed tomography (pQCT), high-resolution peripheral quantitative computed tomography (HR-pQCT), slit-beam digital radiography, and quantitative ultrasound (QUS).

pQCT allows for evaluation of volumetric bone mineral density in the peripheral rather than the axial skeleton, can separately quantify trabecular and cortical volumetric bone mineral density, and has been used in several clinical studies involving OI therapy (43-45). HR-pQCT can further assess bone geometry, volumetric bone mineral density (separately quantifying trabecular and cortical volumetric bone mineral density) and microarchitecture in the peripheral skeleton, and has been used in several clinical studies involving OI therapy (46-53). A slit-beam digital radiography system allows for simultaneous acquisition of tangential images of the entire body with three-dimensional reconstructions, allowing for assessment of skeletal alignment and deformity (54). QUS may have a useful role in the evaluation of patients with OI in the future, particularly in geographical areas where other imaging modalities are not available; however, QUS data is currently scarce. QUS attempts to measure bone quality and bone mass (55, 56).

Conclusion

OI comprises a heterogeneous group of genetic disorders responsible for bone fragility and additional connective tissue disorders. The osseous hallmarks of this “brittle bone disease” can affect any collagen containing structures resulting in frequent fractures, ligamentous hyperlaxity, and neurologic and cardiovascular abnormalities. Differentiating OI from NAT can cause significant consternation, and correlation with family history and presence of non-skeletal manifestations of OI may aide in diagnosis.

Acknowledgements: Fetal MR image courtesy of Katherine Epstein, MD.

Authors' Contributions: Conception and design: JSW and JWR; Acquisition, analysis and interpretation of data: JSW, JWR and SW; Drafting the article: JSW, JWR, SW, JME, MR and BW; Revising it critically for important intellectual content: JSW, JWR and SW; Approved final version of the manuscript: JSW, JWR, SW, JME, MR and BW.

Conflict of Interest: The authors declare that they have no conflict of interest.

References

- Rauch F, Glorieux FH. Osteogenesis imperfecta. *Lancet*. 2004;363(9418):1377-85.
- Körkkö J, Ala-Kokko L, De Paepe A, Nuytinck L, Earley J, Prockop DJ. Analysis of the COL1A1 and COL1A2 genes by PCR amplification and scanning by conformation-sensitive gel electrophoresis identifies only COL1A1 mutations in 15 patients with osteogenesis imperfecta type I: identification of common sequences of null-allele mutations. *Am J Hum Genet*. 1998;62(1):98-110.
- Ralston SH, Gaston MS. Management of Osteogenesis Imperfecta. *Front Endocrinol (Lausanne)*. 2019;10:924.
- Varga P, Willie BM, Stephan C, Kozloff KM, Zysset PK. Finite element analysis of bone strength in osteogenesis imperfecta. *Bone*. 2020;133:115250.
- Wagermaier W, Klaushofer K, Fratzl P. Fragility of Bone Material Controlled by Internal Interfaces. *Calcif Tissue Int*. 2015;97(3):201-12.
- Pezzuti IL, Kakehasi AM, Filgueiras MT, de Guimarães JA, de Lacerda IAC, Silva IN. Imaging methods for bone mass evaluation during childhood and adolescence: an update. *J Pediatr Endocrinol Metab*. 2017;30(5):485-97.
- Mehany SN, Patsch JM. Imaging of pediatric bone and growth disorders: Of diagnostic workhorses and new horizons. *Wien Med Wochenschr*. 2021;171(5-6):102-10.
- Sillence DO, Senn A, Danks DM. Genetic heterogeneity in osteogenesis imperfecta. *J Med Genet*. 1979;16(2):101-16.
- Bonafe L, Cormier-Daire V, Hall C, Lachman R, Mortier G, Mundlos S, et al. Nosology and classification of genetic skeletal disorders: 2015 revision. *Am J Med Genet A*. 2015;167a(12):2869-92.
- Mortier GR, Cohn DH, Cormier-Daire V, Hall C, Krakow D, Mundlos S, et al. Nosology and classification of genetic skeletal disorders: 2019 revision. *Am J Med Genet A*. 2019;179(12):2393-419.
- Rauch F, Fahiminiya S, Majewski J, Carrot-Zhang J, Boudko S, Glorieux F, et al. Cole-Carpenter syndrome is caused by a heterozygous missense mutation in P4HB. *Am J Hum Genet*. 2015;96(3):425-31.
- Parilla BV, Leeth EA, Kambich MP, Chilis P, MacGregor SN. Antenatal detection of skeletal dysplasias. *J Ultrasound Med*. 2003;22(3):255-8; quiz 259-61.
- Thompson EM. Non-invasive prenatal diagnosis of osteogenesis imperfecta. *Am J Med Genet*. 1993;45(2):201-6.
- Fotiadou AN, Calleja M, Hargunani R, Keen R. Skeletal Manifestations of Osteogenesis Imperfecta. *Semin Musculoskelet Radiol*. 2016;20(3):279-86.
- Tsai PY, Chang CH, Yu CH, Cheng YC, Chang FM. Three-dimensional ultrasound in the prenatal diagnosis of osteogenesis imperfecta. *Taiwan J Obstet Gynecol*. 2012;51(3):387-92.
- Nelson DB, Dashe JS, McIntire DD, Twickler DM. Fetal skeletal dysplasias: sonographic indices associated with adverse outcomes. *J Ultrasound Med*. 2014;33(6):1085-90.
- Yoshimura S, Masuzaki H, Gotoh H, Fukuda H, Ishimaru T. Ultrasonographic prediction of lethal pulmonary hypoplasia: comparison of eight different ultrasonographic parameters. *Am J Obstet Gynecol*. 1996;175(2):477-83.
- Renaud A, Aucourt J, Weill J, Bigot J, Dieux A, Devisme L, et al. Radiographic features of osteogenesis imperfecta. *Insights Imaging*. 2013;4(4):417-29.
- Buyse M, Bull MJ. A syndrome of osteogenesis imperfecta, microcephaly, and cataracts. *Birth Defects Orig Artic Ser*. 1978;14(6b):95-8.
- Bronshtein M, Weiner Z. Anencephaly in a fetus with osteogenesis imperfecta: early diagnosis by transvaginal sonography. *Prenat Diagn*. 1992;12(10):831-4.
- Ruano R, Picone O, Benachi A, Grebille AG, Martinovic J, Dumez Y, et al. First-trimester diagnosis of osteogenesis imperfecta associated with encephalocele by conventional and three-dimensional ultrasound. *Prenat Diagn*. 2003;23(7):539-42.

22. Ablin DS, Greenspan A, Reinhart M, Grix A. Differentiation of child abuse from osteogenesis imperfecta. *AJR Am J Roentgenol.* 1990;154(5):1035-46.
23. Brizola E, Zambrano MB, Pinheiro BS, Vanz AP, Félix TM. CLINICAL FEATURES AND PATTERN OF FRACTURES AT THE TIME OF DIAGNOSIS OF OSTEOGENESIS IMPERFECTA IN CHILDREN. *Rev Paul Pediatr.* 2017;35(2):171-7.
24. Wekre LL, Eriksen EF, Falch JA. Bone mass, bone markers and prevalence of fractures in adults with osteogenesis imperfecta. *Arch Osteoporos.* 2011;6(1):31-8.
25. Hui PK, Tung JY, Lam WW, Chau MT. Osteogenesis imperfecta type V. *Skeletal Radiol.* 2011;40(12):1609, 1633.
26. Obafemi AA, Bulas DI, Troendle J, Marini JC. Popcorn calcification in osteogenesis imperfecta: incidence, progression, and molecular correlation. *Am J Med Genet A.* 2008;146a(21):2725-32.
27. Al Muderis M, Azzopardi T, Cundy P. Zebra lines of pamidronate therapy in children. *J Bone Joint Surg Am.* 2007;89(7):1511-6.
28. Corsi A, Ippolito E, Robey PG, Riminucci M, Boyde A. Bisphosphonate-induced zebra lines in fibrous dysplasia of bone: histo-radiographic correlation in a case of McCune-Albright syndrome. *Skeletal Radiol.* 2017;46(10):1435-9.
29. Rauch F, Travers R, Munns C, Glorieux FH. Sclerotic metaphyseal lines in a child treated with pamidronate: histomorphometric analysis. *J Bone Miner Res.* 2004;19(7):1191-3.
30. Schenk R, Merz WA, Mühlbauer R, Russell RG, Fleisch H. Effect of ethane-1-hydroxy-1,1-diphosphonate (EHDP) and dichloromethylene diphosphonate (Cl 2 MDP) on the calcification and resorption of cartilage and bone in the tibial epiphysis and metaphysis of rats. *Calcif Tissue Res.* 1973;11(3):196-214.
31. van Persijn van Meerten EL, Kroon HM, Papapoulos SE. Epi- and metaphyseal changes in children caused by administration of bisphosphonates. *Radiology.* 1992;184(1):249-54.
32. Heimert TL, Lin DD, Yousem DM. Case 48: osteogenesis imperfecta of the temporal bone. *Radiology.* 2002;224(1):166-70.
33. Lonergan GJ, Baker AM, Morey MK, Boos SC. From the archives of the AFIP. Child abuse: radiologic-pathologic correlation. *Radiographics.* 2003;23(4):811-45.
34. Offiah A, van Rijn RR, Perez-Rossello JM, Kleinman PK. Skeletal imaging of child abuse (non-accidental injury). *Pediatr Radiol.* 2009;39(5):461-70.
35. Kempe CH, Helfer RE. *The Battered Child.* 3rd ed. Chicago: University of Chicago Press; 1983.
36. Lafage-Proust MH, Courtois I. The management of osteogenesis imperfecta in adults: state of the art. *Joint Bone Spine.* 2019;86(5):589-93.
37. Roberts TT, Cepela DJ, Uhl RL, Lozman J. Orthopaedic Considerations for the Adult With Osteogenesis Imperfecta. *J Am Acad Orthop Surg.* 2016;24(5):298-308.
38. Tosi LL, Oetgen ME, Floor MK, Huber MB, Kennelly AM, McCarter RJ, et al. Initial report of the osteogenesis imperfecta adult natural history initiative. *Orphanet J Rare Dis.* 2015;10:146.
39. McKiernan FE. Musculoskeletal manifestations of mild osteogenesis imperfecta in the adult. *Osteoporos Int.* 2005;16(12):1698-702.
40. Hald JD, Folkestad L, Swan CZ, Wanscher J, Schmidt M, Gjørup H, et al. Osteogenesis imperfecta and the teeth, eyes, and ears—a study of non-skeletal phenotypes in adults. *Osteoporos Int.* 2018;29(12):2781-9.
41. Hermie I, Horvath M, Van Cauter S. Temporal Bone Imaging Features in Osteogenesis Imperfecta. *J Belg Soc Radiol.* 2017;101(1):27.
42. Radunovic Z, Wekre LL, Diep LM, Steine K. Cardiovascular abnormalities in adults with osteogenesis imperfecta. *Am Heart J.* 2011;161(3):523-9.
43. Rauch F, Cornibert S, Cheung M, Glorieux FH. Long-bone changes after pamidronate discontinuation in children and adolescents with osteogenesis imperfecta. *Bone.* 2007;40(4):821-7.
44. Rauch F, Land C, Cornibert S, Schoenau E, Glorieux FH. High and low density in the same bone: a study on children and adolescents with mild osteogenesis imperfecta. *Bone.* 2005;37(5):634-41.
45. Rauch F, Munns CF, Land C, Cheung M, Glorieux FH. Risedronate in the treatment of mild pediatric osteogenesis imperfecta: a randomized placebo-controlled study. *J Bone Miner Res.* 2009;24(7):1282-9.
46. Fennimore DJ, Digby M, Paggiosi M, Arundel P, Bishop NJ, Dimitri P, et al. High-resolution peripheral quantitative computed tomography in children with osteogenesis imperfecta. *Pediatr Radiol.* 2020;50(12):1781-7.
47. Folkestad L, Hald JD, Hansen S, Gram J, Langdahl B, Abrahamsen B, et al. Bone geometry, density, and microarchitecture in the distal radius and tibia in adults with osteogenesis imperfecta type I assessed by high-resolution pQCT. *J Bone Miner Res.* 2012;27(6):1405-12.
48. Hald JD, Folkestad L, Harsløf T, Lund AM, Duno M, Jensen JB, et al. Skeletal phenotypes in adult patients with osteogenesis imperfecta—correlations with COL1A1/COL1A2 genotype and collagen structure. *Osteoporos Int.* 2016;27(11):3331-41.
49. Kocijan R, Muschitz C, Haschka J, Hans D, Nia A, Geroldinger A, et al. Bone structure assessed by HR-pQCT, TBS and DXL in adult patients with different types of osteogenesis imperfecta. *Osteoporos Int.* 2015;26(10):2431-40.
50. Mikolajewicz N, Zimmermann EA, Rummeler M, Hossainitatabaie S, Julien C, Glorieux FH, et al. Multisite

- longitudinal calibration of HR-pQCT scanners and precision in osteogenesis imperfecta. *Bone*. 2021;147:115880.
51. Plachel F, Renner U, Kocijan R, Muschitz C, Lomoschitz F, Resch H. Osteogenesis imperfecta type III and hypogonadotropic hypogonadism result in severe bone loss: a case report. *Wien Med Wochenschr*. 2015;165(13-14):285-9.
52. Rolvien T, Stürznickel J, Schmidt FN, Butscheidt S, Schmidt T, Busse B, et al. Comparison of Bone Microarchitecture Between Adult Osteogenesis Imperfecta and Early-Onset Osteoporosis. *Calcif Tissue Int*. 2018;103(5):512-21.
53. Schanda JE, Huber S, Behanova M, Haschka J, Kraus DA, Meier P, et al. Analysis of bone architecture using fractal-based TX-Analyzer™ in adult patients with osteogenesis imperfecta. *Bone*. 2021;147:115915.
54. Melhem E, Assi A, El Rachkidi R, Ghanem I. EOS(®) biplanar X-ray imaging: concept, developments, benefits, and limitations. *J Child Orthop*. 2016;10(1):1-14.
55. Cepollaro C, Gonnelli S, Pondrelli C, Montagnani A, Martini S, Bruni D, et al. Osteogenesis imperfecta: bone turnover, bone density, and ultrasound parameters. *Calcif Tissue Int*. 1999;65(2):129-32.
56. Kutilek S, Bayer M. Quantitative ultrasonometry of the calcaneus in children with osteogenesis imperfecta. *J Paediatr Child Health*. 2010;46(10):592-4.